

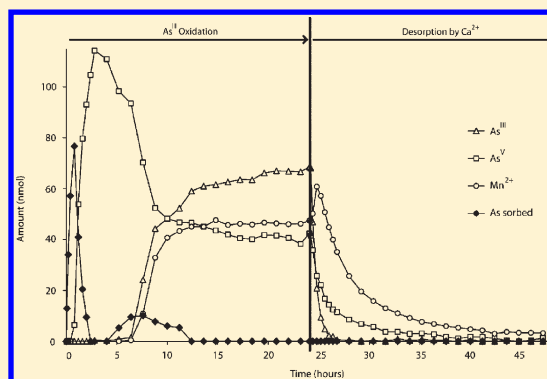
## Arsenite Oxidation by a Poorly-Crystalline Manganese Oxide. 3. Arsenic and Manganese Desorption

Brandon J. Lafferty,<sup>\*,†</sup> Matthew Ginder-Vogel,<sup>‡</sup> and Donald L. Sparks

Department of Plant and Soil Sciences, Delaware Environmental Institute, University of Delaware, 152 Townsend Hall, Newark, Delaware 19716, United States

**S** Supporting Information

**ABSTRACT:** Arsenic (As) mobility in the environment is greatly affected by its oxidation state and the degree to which it is sorbed on metal oxide surfaces. Manganese oxides (Mn oxides) have the ability to decrease overall As mobility both by oxidizing toxic arsenite ( $\text{As}^{\text{III}}$ ) to less toxic arsenate ( $\text{As}^{\text{V}}$ ), and by sorbing As. However, the effect of competing ions on the mobility of As sorbed on Mn-oxide surfaces is not well understood. In this study, desorption of  $\text{As}^{\text{V}}$  and  $\text{As}^{\text{III}}$  from a poorly crystalline phylломanganate ( $\delta\text{-MnO}_2$ ) by two environmentally significant ions is investigated using a stirred-flow technique and X-ray absorption spectroscopy (XAS).  $\text{As}^{\text{III}}$  is not observed in solution after desorption under any conditions used in this study, agreeing with previous studies showing As sorbed on Mn-oxides exists only as  $\text{As}^{\text{V}}$ . However, some  $\text{As}^{\text{V}}$  is desorbed from the  $\delta\text{-MnO}_2$  surface under all conditions studied, while neither desorptive used in this study completely removes  $\text{As}^{\text{V}}$  from the  $\delta\text{-MnO}_2$  surface.



### INTRODUCTION

Arsenic (As) is an element with toxic properties, commonly found in the environment. Elevated As levels in soils result from both natural weathering processes and anthropogenic activities such as mining, agriculture, and manufacturing.<sup>1</sup> In several locations throughout the world, As contamination of soil and water occurs near human populations, posing a significant threat to human health. Therefore, understanding the chemical reactions controlling As mobility in the environment is critical.

Arsenic behavior in the environment is significantly determined by its chemical speciation. Usually, As occurs as one of two inorganic oxyanions: arsenite ( $\text{As}^{\text{III}}$ ) or arsenate ( $\text{As}^{\text{V}}$ ). Below pH 9,  $\text{As}^{\text{III}}$  appears predominately in its fully protonated form ( $\text{H}_3\text{AsO}_3$ ), while at circumneutral pH values,  $\text{As}^{\text{V}}$  occurs as a mixture of  $\text{H}_2\text{AsO}_4^-$  and  $\text{HAsO}_4^{2-}$ . Arsenic speciation also determines its toxicity because  $\text{As}^{\text{III}}$  is more toxic than  $\text{As}^{\text{V}}$ .<sup>3</sup> Several Mn-oxides can readily oxidize  $\text{As}^{\text{III}}$  to  $\text{As}^{\text{V}}$ , most notably layered Mn-oxides (i.e., phylломanganates),<sup>4–14</sup> thus Mn-oxide minerals can have a determining effect on As speciation in soils and sediments.

In terrestrial environments, As mobility is generally determined by the extent to which it is adsorbed by metal oxides.<sup>15–21</sup> Phylломanganates represent one type of metal oxide that exhibit the ability to sorb As.<sup>6,11,12,22–25</sup> However, sorption of As on Mn-oxide surfaces can be quite complex. Interestingly, a higher level of As sorption has been observed when  $\text{As}^{\text{III}}$  is reacted with phylломanganates (oxidation and sorption) compared to reaction of  $\text{As}^{\text{V}}$  with phylломanganates (sorption alone).<sup>4,6,11,23,25</sup> Also, when  $\text{As}^{\text{V}}$  is sorbed on Mn-oxide surfaces, it forms a variety of surface complexes.<sup>14,22–24</sup>

Since Mn-oxides have shown a propensity to oxidize and sorb As in nature, it is important to understand potential mobility of As adsorbed on Mn-oxide surfaces. Because  $\text{As}^{\text{V}}$  forms multiple surface complexes with Mn-oxides, it is possible that mobility of As sorbed on Mn-oxides varies depending on the surface complexes present. Also, in nature, As coexists with other ions which can compete for sorption sites on Mn-oxide surfaces. Therefore, understanding As mobility in the environment requires understanding the mobility of various As surface complexes, as well as the potential for competing ions to desorb As from Mn-oxide surfaces. To date, few studies have investigated the ability of common environmental ions to desorb As from the surface of Mn-oxides. The purpose of this study is to determine to what extent a cation ( $\text{Ca}^{2+}$ ), and oxyanion ( $\text{H}_2\text{PO}_4^-/\text{HPO}_4^{2-}$ ), both common in the environment, are able to desorb As from a poorly crystalline phylломanganate ( $\delta\text{-MnO}_2$ ).

### MATERIALS AND METHODS

**Stirred Flow Method.** Stirred flow experiments were conducted using the same 30 mL reactor and experimental procedures described previously.<sup>6</sup> All stirred flow reactions were conducted in a background electrolyte (10 mM NaCl), buffered at pH 7.2 (5 mM 3-(N-morpholino)propanesulfonic acid (MOPS)),

**Received:** April 15, 2011

**Accepted:** September 28, 2011

**Revised:** August 9, 2011

**Published:** September 28, 2011

and had a constant flow rate of 1 mL/min. Also, all experiments were mixed via a magnetic stir bar with a constant rate of stirring (100 rpm).

In all desorption reactions, 1 g/L  $\delta$ -MnO<sub>2</sub> was reacted with 100  $\mu$ M As<sup>III</sup> (i.e., As is oxidized and sorbed) to ensure maximum As sorption on the solid phase, followed immediately by reaction with a desorptive. Oxidation of As<sup>III</sup> (and As sorption) prior to desorption was carried out for 4, 10, or 24 h. The desorptives used were 100  $\mu$ M calcium chloride (CaCl<sub>2</sub>, abbreviated Ca<sup>2+</sup>) in the presence of background electrolyte (10 mM NaCl and 5 mM MOPS), 100  $\mu$ M sodium phosphate (NaH<sub>2</sub>PO<sub>4</sub>, abbreviated PO<sub>4</sub>) in the presence of background electrolyte, or background electrolyte alone. All solutions were adjusted to pH 7.2 with HCl and NaOH prior to experiments, and background electrolyte was introduced into the stirred flow reactor (containing  $\delta$ -MnO<sub>2</sub>) for at least 2 h at a rate of 1 mL/min prior to each experiment. In each reaction, As<sup>III</sup> oxidation was stopped (after 4, 10, or 24 h) by introducing desorbing solution into the reactor, thus beginning the desorption phase of the reaction. Changing influent solution from As<sup>III</sup> solution to desorption solution took less than 5 s, and thus flow of solution into the reactor was effectively constant throughout each experiment (oxidation followed by desorption). A plot showing the full data (As<sup>III</sup> oxidation followed by desorption) from one experiment is presented in the Supporting Information (Figure S1).

**As, Mn, Ca, and P Analysis.** Inorganic arsenic in the stirred flow effluent was analyzed via liquid chromatography inductively coupled plasma mass spectrometry (LC-ICP-MS), and aqueous Mn was analyzed by ICP-MS as described in Lafferty et al.<sup>6</sup> Total P and Ca in the reactor effluent were analyzed by ICP-OES to verify the concentration of desorptive present in the stirred-flow reactor (data not shown).

**EXAFS Analysis.** Extended X-ray absorption fine structure (EXAFS) spectroscopic analysis was performed at the National Synchrotron Light Source (Brookhaven National Laboratory) on reacted  $\delta$ -MnO<sub>2</sub> after 24 h of desorption (following reaction with 100  $\mu$ M As<sup>III</sup> for 4, 10, and 24 h). Detailed descriptions of sample collection, data collection and data processing for samples analyzed using these techniques can be found in the Supporting Information.

**Sorption and Desorption Calculations.** To quantify the total amount of sorbed and desorbed As<sup>V</sup>, As<sup>III</sup>, and Mn<sup>2+</sup> data were integrated using the “area below curves” tool in SigmaPlot 8 (Systat Software Inc., San Jose, California).

## RESULTS AND DISCUSSION

**$\delta$ -MnO<sub>2</sub> Structure.** Mineral structure must be taken into consideration in order to accurately interpret adsorption and desorption data. The  $\delta$ -MnO<sub>2</sub> used in this study is a poorly ordered form of hexagonal birnessite.<sup>24</sup> Hexagonal birnessite (and thus  $\delta$ -MnO<sub>2</sub>) has two types of reactive sites: at vacancies within Mn<sup>IV</sup> octahedral sheets (vacancy sites) and at the edges of Mn<sup>IV</sup> octahedral sheets (edge sites).<sup>26,27</sup> It has been shown that As reacts primarily with edge sites, rather than vacancy sites of birnessite;<sup>14,23,24</sup> therefore, in this study, As desorption is expected to occur at  $\delta$ -MnO<sub>2</sub> edge sites. However, heavy metals tend to sorb strongly at phyllosmanganate vacancy sites,<sup>26–33</sup> as well as react with edge sites of phyllosmanganates.<sup>31,34</sup> Because of the high affinity of vacancy sites for Mn<sup>2+</sup>, vacancy sites are likely the primary location of Mn<sup>2+</sup> sorption on  $\delta$ -MnO<sub>2</sub>, however, once  $\delta$ -MnO<sub>2</sub> vacancy sites begin to fill, Mn<sup>2+</sup> is expected to react

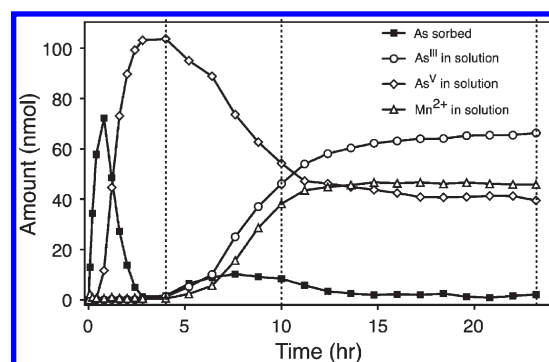
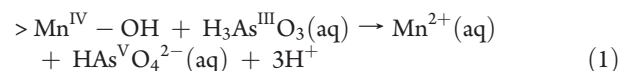


**Figure 1.** The amount (nmol) of As<sup>III</sup>, As<sup>V</sup>, and Mn<sup>2+</sup> in stirred flow reactor effluent as well as the amount (nmol) of As sorbed during As<sup>III</sup> oxidation by  $\delta$ -MnO<sub>2</sub>, prior to desorption by Ca<sup>2+</sup>, PO<sub>4</sub>, or background electrolyte. Vertical dashed lines indicate times for which desorption was initiated.

more with  $\delta$ -MnO<sub>2</sub> edge sites.<sup>6,24</sup> Therefore, in these experiments, desorption of Mn<sup>2+</sup> is expected to occur at both edge and vacancy sites of  $\delta$ -MnO<sub>2</sub> depending on the extent to which  $\delta$ -MnO<sub>2</sub> vacancy sites are filled with Mn<sup>2+</sup>. A graphic representation of As and Mn sorption on the  $\delta$ -MnO<sub>2</sub> surface can be found in Figure 4 of Lafferty et al.<sup>24</sup>

**As<sup>III</sup> Oxidation and Sorption.** All desorption experiments in this study are preceded by reaction of As<sup>III</sup> with  $\delta$ -MnO<sub>2</sub> for 4, 10, or 24 h. This initial reaction between As<sup>III</sup> and  $\delta$ -MnO<sub>2</sub> results in As<sup>III</sup> oxidation and produces As<sup>V</sup> and Mn<sup>2+</sup> (eq 1). Subsequently, As<sup>V</sup> and Mn<sup>2+</sup> produced during As<sup>III</sup> oxidation are sorbed on the  $\delta$ -MnO<sub>2</sub> surface.



To briefly summarize Lafferty et al.,<sup>6,24</sup> the reaction between As<sup>III</sup> and  $\delta$ -MnO<sub>2</sub> in a stirred-flow reactor, under the conditions used in this study, proceeds in two distinct phases. First, an initial reaction phase occurs from 0 to 6.4 h, which includes the period of fastest As<sup>III</sup> oxidation, highest As<sup>V</sup> sorption, and no Mn<sup>2+</sup> release into solution (Figure 1). A second reaction phase characterized by lower  $\delta$ -MnO<sub>2</sub> reactivity occurs beyond 6.4 h, which includes a second period of (decreased) As sorption, a decrease in As<sup>III</sup> oxidation rate, and the presence of Mn<sup>2+</sup> in solution (Figure 1). Decreased  $\delta$ -MnO<sub>2</sub> reactivity in the second phase of this reaction has been attributed to Mn<sup>2+</sup> sorption on the  $\delta$ -MnO<sub>2</sub> surface and the subsequent production of Mn<sup>III</sup> via Mn(II)/(IV) conproportionation at the  $\delta$ -MnO<sub>2</sub> surface.<sup>24</sup>

In this study, desorption experiments are conducted by stopping the initial reaction between As<sup>III</sup> and  $\delta$ -MnO<sub>2</sub> after 4, 10, or 24 h (Figure 1), and simultaneously beginning desorption by PO<sub>4</sub>, Ca<sup>2+</sup>, or background electrolyte alone. The first time point for beginning desorption is after 4 h of reaction between As<sup>III</sup> and  $\delta$ -MnO<sub>2</sub>, which coincides with maximum As<sup>V</sup> concentration in the stirred-flow reactor effluent, and the end of an initial period of As<sup>V</sup> sorption (Figure 1). Between 0 and 4 h of As<sup>III</sup> oxidation, Mn<sup>2+</sup> is expected to react primarily with vacancy sites and not edge sites. The second time point for beginning desorption is after 10 h of As<sup>III</sup> oxidation by  $\delta$ -MnO<sub>2</sub>, which is near the end of a second period of lesser As sorption, and occurs early in the second, less reactive phase of As<sup>III</sup> oxidation (Figure 1). Between 4 and 10 h, Mn<sup>2+</sup> is expected to begin reacting with edge sites, resulting in formation of some Mn<sup>III</sup>.<sup>24</sup> A change in the sorption

**Table 1. Structural Parameters Derived from Least-Square Fits to Raw  $k^3$ -Weighted As-EXAFS Spectra for  $\delta$ -MnO<sub>2</sub> after 24 h Desorption by Background Electrolyte (Elec), Calcium Solution (Ca), and Phosphate Solution (PO<sub>4</sub>)<sup>a</sup>**

sample	As–O			As–Mn			As–Mn		
	CN <sup>b</sup>	r <sup>b</sup>	$\sigma^{2b}$	CN <sup>b</sup>	r <sup>b</sup>	$\sigma^{2b}$	CN <sup>b</sup>	r <sup>b</sup>	$\sigma^{2b}$
10 h-elec	4.1(2)	1.70(1)	0.003(0)	1.1(3)	3.12(2)	0.005(1)	0.6(4)	3.50(5)	0.005(3)
10 h-Ca	4.1(2)	1.70(1)	0.003(0)	0.7(4)	3.14(3)	0.005(2)	0.3(5)	3.51(9)	0.004(7)
10 h-PO <sub>4</sub>	4.2(2)	1.70(1)	0.003(0)	0.8(3)	3.16(3)	0.005(2)			
24 h-elec	4.1(1)	1.70(1)	0.003(0)	0.8(3)	3.15(2)	0.005(2)			
24 h-Ca	4.1(1)	1.69(0)	0.003(0)	0.9(3)	3.14(2)	0.005(2)			
24 h-PO <sub>4</sub>	4.3(2)	1.69(0)	0.003(0)	0.7(3)	3.16(3)	0.006(3)			

<sup>a</sup> Desorption data shown here followed 10 or 24 h of As<sup>III</sup> oxidation. <sup>b</sup> Coordination number (CN), interatomic distance (r), and Debye–Waller factor ( $\sigma^2$ ) were obtained by fitting data with theoretical phase and amplitude functions. Estimated errors at 95% confidence interval from the least-squares fit are given in parentheses.

complexes formed between As<sup>V</sup> and  $\delta$ -MnO<sub>2</sub> also occurs between 4 and 10 h of As<sup>III</sup> oxidation.<sup>24</sup> The last time point for desorption is after 24 h of reaction, when the system is stable within the less reactive phase of the reaction (Figure 1).

**As<sup>III</sup> Desorption.** No As<sup>III</sup> is desorbed from the  $\delta$ -MnO<sub>2</sub> surface in any desorption experiments discussed here. Also, As EXAFS analysis indicates that all As associated with  $\delta$ -MnO<sub>2</sub> after desorption is present as As<sup>V</sup> (Table 1 and Figures 2 and 3), which agrees with previous results indicating that As present on phyllo-manganate surfaces only occurs as As<sup>V</sup>.<sup>14,23,24,35</sup> However, it should be noted that there is not a sufficient amount of As remaining on the surface of  $\delta$ -MnO<sub>2</sub> after 4 h of As<sup>III</sup> oxidation followed by 24 h of desorption to measure As using EXAFS analysis.

**As<sup>V</sup> Desorption.** Previous studies have shown that As reacts primarily with edge sites of phyllo-manganates rather than vacancy sites,<sup>14,23,24</sup> therefore As<sup>V</sup> desorption in this study is expected to occur at  $\delta$ -MnO<sub>2</sub> edge sites. Of the desorptives used in this study, PO<sub>4</sub> is expected to desorb As<sup>V</sup> most readily because it is chemically similar to As<sup>V</sup> and is known to compete with As<sup>V</sup> for sorption sites on metal oxide minerals.<sup>12,36–38</sup> However, Ca<sup>2+</sup> has the potential to react with  $\delta$ -MnO<sub>2</sub> vacancy sites as well as edge sites, therefore, Ca<sup>2+</sup> also has the potential to desorb As<sup>V</sup>. The background electrolyte (MOPS and NaCl) used in these studies is expected to react weakly with  $\delta$ -MnO<sub>2</sub> edge sites, and thus should not desorb As<sup>V</sup> to a large extent.

When As<sup>V</sup> is desorbed (for 24 h) after 4 h of As<sup>III</sup> oxidation, roughly 67% of As<sup>V</sup> sorbed during the 4 h of As<sup>III</sup> oxidation is mobilized from the  $\delta$ -MnO<sub>2</sub> surface by all three desorptives (Figure 2). Because of this, one can infer that the majority of As<sup>V</sup> sorbed on the  $\delta$ -MnO<sub>2</sub> surface during the initial phase of high  $\delta$ -MnO<sub>2</sub> reactivity is fairly labile. Conversely, there is a portion of As<sup>V</sup> sorbed during the first 4 h of As<sup>III</sup> oxidation that remains immobile on the  $\delta$ -MnO<sub>2</sub> surface, even in the presence of PO<sub>4</sub>. Previous EXAFS analysis of  $\delta$ -MnO<sub>2</sub> reacted with As<sup>III</sup> under identical experimental conditions revealed that As<sup>V</sup> is bound in mononuclear-monodentate as well as binuclear-bidentate complexes on the  $\delta$ -MnO<sub>2</sub> surface during the first 4 h of As<sup>III</sup> oxidation by  $\delta$ -MnO<sub>2</sub>.<sup>24</sup> Unfortunately, there is not a sufficient amount of As remaining on the surface of  $\delta$ -MnO<sub>2</sub> after 4 h of As<sup>III</sup> oxidation followed by 24 h of desorption to determine the stability of these two complexes by EXAFS analysis.

After 10 and 24 h of As<sup>III</sup> oxidation, PO<sub>4</sub> is a more efficient desorptive of As<sup>V</sup> than Ca<sup>2+</sup> or the background electrolyte (Figure 2). Also, the proportion of As<sup>V</sup> desorbed by PO<sub>4</sub>

increases in the 10 and 24 h experiments (Figure 2). It should be noted that after 10 and 24 h of As<sup>III</sup> oxidation by  $\delta$ -MnO<sub>2</sub>, two significant changes occur in the speciation of Mn associated with  $\delta$ -MnO<sub>2</sub>. First, Mn<sup>2+</sup> begins sorbing at edge sites after  $\delta$ -MnO<sub>2</sub> vacancy sites are occupied by sorbed Mn<sup>2+</sup> (at  $\sim$ 6.4 h).<sup>6,24</sup> Also, Mn<sup>III</sup> begins to appear in Mn octahedral layers of  $\delta$ -MnO<sub>2</sub> between 4 and 10 h of As<sup>III</sup> oxidation, and increases between 10 and 24 h.<sup>24</sup> An increase in the proportion of As<sup>V</sup> desorbed by all desorptives after 10 and 24 h (compared to 4 h) happens concurrently with increased competition from Mn<sup>2+</sup> for edge sites, and an increase in Mn<sup>III</sup> content within the  $\delta$ -MnO<sub>2</sub> structure. Thus, increased As<sup>V</sup> desorption in the 10 and 24 h experiments could be the result of direct competition between As<sup>V</sup> and Mn<sup>2+</sup> for sorption sites or the formation of weaker bonds between As<sup>V</sup> and Mn<sup>III</sup>.<sup>39</sup> It is difficult to distinguish between the effects of increased Mn<sup>2+</sup> sorption and increased Mn<sup>III</sup> content at  $\delta$ -MnO<sub>2</sub> edge sites as they occur simultaneously.

EXAFS analysis of  $\delta$ -MnO<sub>2</sub> after As<sup>III</sup> oxidation for 10 h and subsequent desorption by Ca<sup>2+</sup> and background electrolyte revealed As–Mn distances of  $\sim$ 3.13 Å and  $\sim$ 3.50 Å (Table 1). These distances correspond to As<sup>V</sup> bound to the  $\delta$ -MnO<sub>2</sub> surface in bidentate-binuclear and monodentate-mononuclear complexes, respectively.<sup>22–24</sup> However, for all other desorption experiments after 10 (PO<sub>4</sub>) and 24 (Ca<sup>2+</sup>, PO<sub>4</sub>, and background electrolyte) hours of As<sup>III</sup> oxidation by  $\delta$ -MnO<sub>2</sub> the only As–Mn distances present in EXAFS spectra was  $\sim$ 3.15 Å (Table 1 and Figure 3), corresponding to a bidentate-binuclear complex between As<sup>V</sup> and the  $\delta$ -MnO<sub>2</sub> surface. While, it is tenuous to attribute a specific desorption event with a single adsorption complex, EXAFS data of As sorption complexes before and after desorption seem to indicate that bidentate-mononuclear and monodentate-mononuclear complexes between As<sup>V</sup> and the  $\delta$ -MnO<sub>2</sub> surface are less stable than As<sup>V</sup>- $\delta$ -MnO<sub>2</sub> bidentate-binuclear complexes.

**Mn Desorption.** During As<sup>III</sup> oxidation by  $\delta$ -MnO<sub>2</sub>, Mn<sup>2+</sup> is produced and subsequently sorbed by  $\delta$ -MnO<sub>2</sub> (eq 1 and Figure 1).<sup>6,24</sup> Mn<sup>2+</sup> tends to initially sorb at  $\delta$ -MnO<sub>2</sub> layer vacancy sites under the conditions used in this study, followed by sorption at  $\delta$ -MnO<sub>2</sub> edge sites as vacancy sites become more occupied.<sup>24</sup> Previous studies have indicated that some As sorbed on phyllo-manganate surfaces could be bound through a bridging complex through sorbed Mn.<sup>12,25</sup> Although As/ $\delta$ -MnO<sub>2</sub> bridging complexes were not seen in previous studies conducted under the experimental conditions used in the reactions described here, it is possible that Mn<sup>2+</sup> on  $\delta$ -MnO<sub>2</sub> could facilitate As sorption.

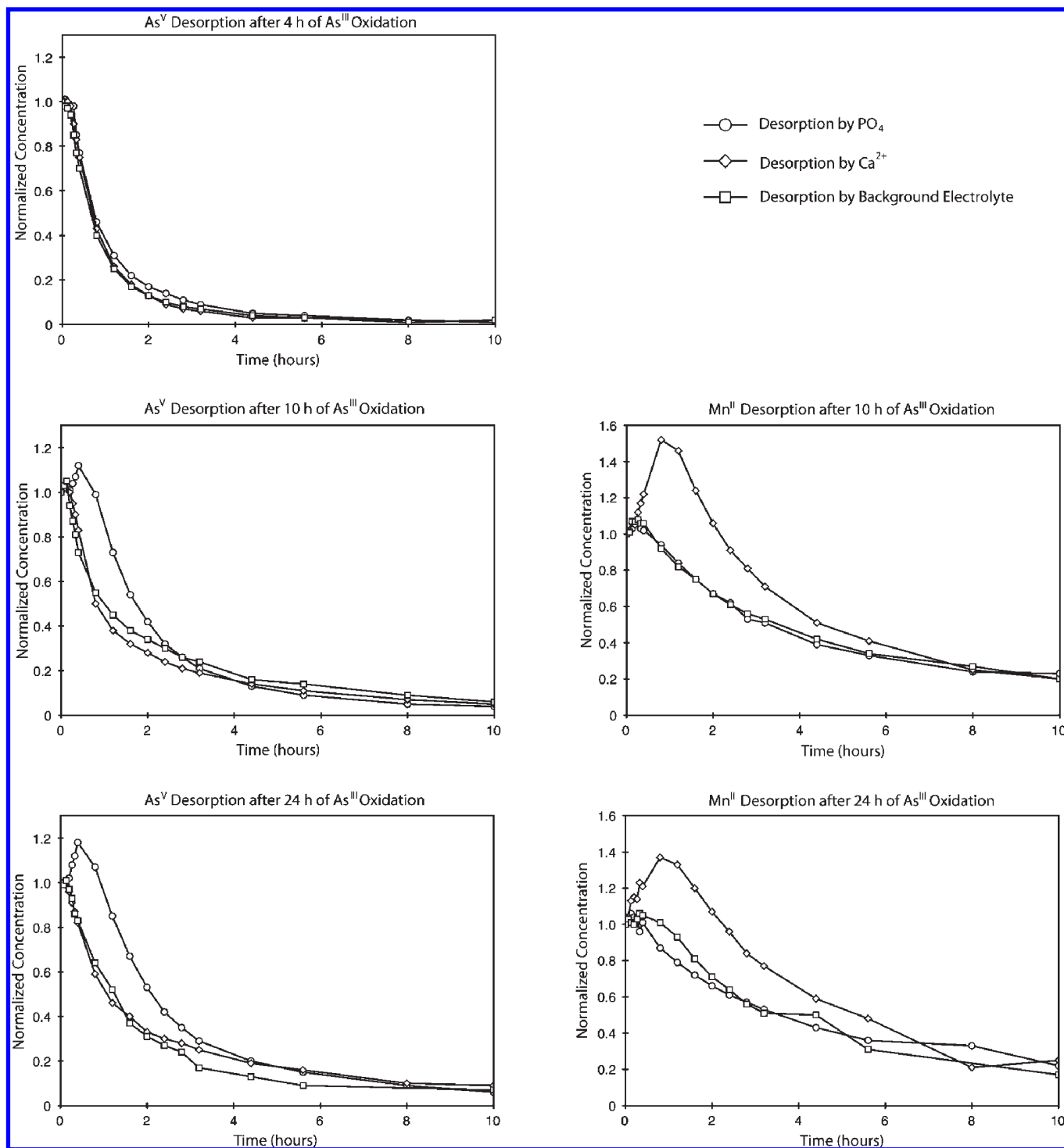


**Figure 2.** As<sup>V</sup> (left) and Mn<sup>2+</sup> (right) desorbed by Ca<sup>2+</sup>, PO<sub>4</sub>, and background electrolyte (10 mM NaCl, 5 mM MOPS) after As<sup>III</sup> oxidation by  $\delta$ -MnO<sub>2</sub>. The initial data points on each graph (time = 0 h) correspond to the beginning of desorption (initial As<sup>III</sup> oxidation data not shown). Data shown are first 10 h of 24 h desorption experiments.

Of the desorptives used in this study, Ca<sup>2+</sup> is expected to react with  $\delta$ -MnO<sub>2</sub> sorption sites most similarly to Mn<sup>2+</sup>.<sup>40</sup> Some cations could potentially desorb Mn<sup>2+</sup> more readily than Ca<sup>2+</sup>,<sup>32,41,42</sup> however Ca<sup>2+</sup> is ubiquitous in nature, and thus has a high probability of interacting with Mn<sup>2+</sup> sorbed on Mn-oxide surfaces. Desorption of Mn<sup>2+</sup> by Na<sup>+</sup> (in background electrolyte) is predicted to be negligible because Na<sup>+</sup> reacts with  $\delta$ -MnO<sub>2</sub>

interlayers differently than Ca<sup>2+</sup> or Mn<sup>2+</sup>, in that Na<sup>+</sup> is not expected to bind in triple corner sharing complexes at vacancy sites as is the case with Mn<sup>2+</sup> and Ca<sup>2+</sup>.<sup>40</sup>

When As<sup>III</sup> is reacted with  $\delta$ -MnO<sub>2</sub> for only 4 h, no Mn<sup>2+</sup> is desorbed under the conditions used in this study (data not shown). It is important to note that no Mn<sup>2+</sup> appears in the stirred-flow reactor effluent during the first 4 h of As<sup>III</sup> oxidation, and all Mn<sup>2+</sup>

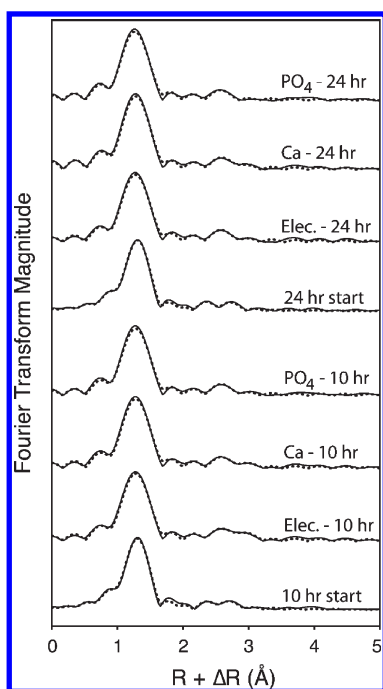


**Figure 3.** Fourier transformed As K-edge EXAFS of  $\delta$ -MnO<sub>2</sub> reacted with As<sup>III</sup> (100  $\mu$ M) in a stirred-flow reactor for 10 and 24 h (10 h start and 24 h start) and desorbed by Ca<sup>2+</sup>, PO<sub>4</sub>, and background electrolyte for 24 h following As<sup>III</sup> reaction. XAS data are presented as solid lines and fits are presented as dashed lines (fit data provided in Table 1).

produced during this time is expected to sorb strongly at  $\delta$ -MnO<sub>2</sub> vacancy sites.<sup>24</sup> However, after 10 and 24 h of As<sup>III</sup> oxidation, Mn<sup>2+</sup> is desorbed by all desorptives studied (Figure 2), indicating that Mn<sup>2+</sup> sorbed at  $\delta$ -MnO<sub>2</sub> edge sites is more labile than Mn<sup>2+</sup> sorbed at  $\delta$ -MnO<sub>2</sub> vacancy sites. Mn EXAFS analysis of  $\delta$ -MnO<sub>2</sub> revealed no detectable changes in Mn speciation of the solid material after desorption which would appear as a broadening and decrease in the peak height of the 9.25  $\text{\AA}^{-1}$  peak in the EXAFS spectra<sup>24</sup> (Figures S2A and S2B and Table S1 of the Supporting Information, SI). As predicted, Ca<sup>2+</sup> is the most efficient Mn<sup>2+</sup> desorptive of those studied. The proportion of Mn<sup>2+</sup> desorbed by Ca<sup>2+</sup> is greatest after 10 h of As<sup>III</sup> oxidation and decreases slightly after 24 h of As<sup>III</sup> oxidation (Figure 2). This decrease in Mn<sup>2+</sup> mobility with increased As<sup>III</sup> oxidation time could potentially be due to increased formation of less mobile Mn<sup>III</sup> after 10 h of reaction.<sup>6,24</sup> Also, desorption by PO<sub>4</sub> (with background electrolyte present) is nearly identical to desorption by background electrolyte alone in the 10 and 24 h samples (Figure 2), which suggests that PO<sub>4</sub> does not desorb Mn<sup>2+</sup> appreciably. Interestingly, increased Mn<sup>2+</sup> desorption by Ca<sup>2+</sup> compared to other desorptives does not result in an increase in As<sup>V</sup> desorption, which provides some evidence that As<sup>V</sup> is not bound to the  $\delta$ -MnO<sub>2</sub> surface via a bridging complex through Mn<sup>2+</sup>.

**Implications for As Mobility.** Phyllosulfates are capable of sorbing As<sup>V</sup>, especially during As<sup>III</sup> oxidation. However, in this study, As<sup>V</sup> can be desorbed from the  $\delta$ -MnO<sub>2</sub> surface, to some extent, under all conditions studied. Even Na<sup>+</sup> (present in background electrolyte) is able to desorb As<sup>V</sup>, to some extent, under all conditions studied here, indicating that a portion of As sorbed by Mn-oxides is potentially quite mobile in the environment. Although some sorbed As<sup>V</sup> can be desorbed from  $\delta$ -MnO<sub>2</sub>, there

is a certain amount of As that is not desorbed under any of the conditions studied here. Thus, if As comes in contact with Mn-oxides in nature, these minerals could potentially decrease As availability and mobility both by oxidation of As<sup>III</sup> and sorption of As<sup>V</sup>. It appears that As<sup>V</sup> and Mn<sup>2+</sup> desorption potential is intricately linked to the type of reaction site on the  $\delta$ -MnO<sub>2</sub> surface to which each is bound, as well as Mn speciation within the  $\delta$ -MnO<sub>2</sub> structure. This study emphasizes the importance of understanding mineral structures and temporal variability when predicting As mobility in the environment.

## ■ ASSOCIATED CONTENT

**S Supporting Information.** Supporting Information is provided which includes detailed information about EXAFS analysis, Mn EXAFS fitting results, further Mn desorption discussion, and an example of aqueous data from a full experiment. This material is available free of charge via the Internet at <http://pubs.acs.org>.

## ■ AUTHOR INFORMATION

### Corresponding Author

\*Phone: (601) 634-3589; fax: (601) 634-4017; e-mail: [blafferty@gmail.com](mailto:blafferty@gmail.com).

### Present Addresses

<sup>†</sup>United States Army Corps of Engineers, Engineer Research and Development Center, 3909 Halls Ferry Rd, Vicksburg, MS 39180.

<sup>‡</sup>Calera Corporation, 14600 Winchester Blvd, Los Gatos, CA 95030.

## ■ ACKNOWLEDGMENT

The authors thank Gerald Hendricks and Caroline Golt for laboratory assistance. B.L. is grateful for funding provided by a University of Delaware graduate fellowship and the Donald L. and Joy G. Sparks Graduate Fellowship in Soil Science. This research was funded by United States Department of Agriculture Grant 2005–35107-16105, National Science Foundation Grant EAR-0544246, and Delaware National Science Foundation EPSCoR Grant EPS-0447610. Use of the National Synchrotron Light Source, Brookhaven National Laboratory, was supported by the U.S. Department of Energy, Office of Science, Office of Basic Energy Sciences, under Contract No. DE-AC02-98CH10886.

## ■ REFERENCES

- (1) Cullen, W. R.; Reimer, K. J. Arsenic speciation in the environment. *Chem. Rev.* **1989**, *89*, 713–764.
- (2) Sadiq, M. Arsenic chemistry in soils: An overview of thermodynamic predictions and field observations. *Water, Air, Soil Pollut.* **1997**, *93*, 117–136.
- (3) Petrick, J. S.; Ayala-Fierro, F.; Cullen, W. R.; Carter, D. E.; Aposthian, H. V. Monomethylarsonous acid (MMA(III)) is more toxic than arsenite in Chang human hepatocytes. *Toxicol. Appl. Pharmacol.* **2000**, *163*, 203–207.
- (4) Driehaus, W.; Seith, R.; Jekel, M. Oxidation of arsenate (III) with manganese oxides in water treatment. *Water Res.* **1995**, *29*, 297–305.
- (5) Ginder-Vogel, M.; Landrot, G.; Fischel, J. S.; Sparks, D. L. Quantification of rapid environmental redox processes with quick-scanning x-ray absorption spectroscopy (Q-XAS). *Proc. Natl. Acad. Sci.* **2009**, *106*, 16124–16128.
- (6) Lafferty, B. J.; Ginder-Vogel, M.; Sparks, D. L. Arsenite oxidation by a poorly crystalline manganese-oxide I. Stirred-flow experiments. *Environ. Sci. Technol.* **2010**, *44*, 8460–8466.

- (7) Moore, J. N.; Walker, J. R.; Hayes, T. H. Reaction scheme for the oxidation of As (III) to As (V) by birnessite. *Clays Clay Miner.* **1990**, *38*, 549–555.
- (8) Nesbitt, H.; Canning, G.; Bancroft, G. XPS study of reductive dissolution of 7Å-birnessite by H<sub>3</sub>AsO<sub>3</sub>, with constraints on reaction mechanism. *Geochim. Cosmochim. Acta* **1998**, *62*, 2097–2110.
- (9) Oscarson, D.; Huang, P.; Defosse, C.; Herbillon, A. Oxidative power of Mn (IV) and Fe (III) oxides with respect to As (III) in terrestrial and aquatic environments. *Nature* **1981**, *291*, 50–51.
- (10) Oscarson, D.; Huang, P.; Liaw, W. Role of manganese in the oxidation of arsenite by freshwater lake sediments. *Clays Clay Miner* **1981**, *29*, 219–225.
- (11) Oscarson, D.; Huang, P.; Hammer, U.; Liaw, W. Oxidation and sorption of arsenite by manganese dioxide as influenced by surface coatings of iron and aluminum oxides and calcium carbonate. *Water, Air, Soil Pollut.* **1983**, *20*, 233–244.
- (12) Parikh, S. J.; Lafferty, B. J.; Meade, T. G.; Sparks, D. L. Evaluating Environmental Influences on As(III) Oxidation Kinetics by a Poorly Crystalline Mn-Oxide. *Environ. Sci. Technol.* **2010**, *44*, 3772–3778.
- (13) Scott, M. J.; Morgan, J. J. Reactions at oxide surfaces. 1. Oxidation of As (III) by synthetic birnessite. *Environ. Sci. Technol.* **1995**, *29*, 1898–1905.
- (14) Tournassat, C.; Charlet, L.; Bosbach, D.; Manceau, A. Arsenic(III) oxidation by birnessite and precipitation of manganese(II) arsenate. *Environ. Sci. Technol.* **2002**, *36*, 493–500.
- (15) Arai, Y.; Elzinga, E. J.; Sparks, D. L. X-ray absorption spectroscopic investigation of arsenite and arsenate adsorption at the aluminum oxide-water interface. *J. Colloid Interface Sci.* **2001**, *235*, 80–88.
- (16) Dixit, S.; Hering, J. G. Comparison of arsenic(V) and arsenic(III) sorption onto iron oxide minerals: Implications for arsenic mobility. *Environ. Sci. Technol.* **2003**, *37*, 4182–4189.
- (17) Raven, K. P.; Jain, A.; Loeppert, R. H. Arsenite and arsenate adsorption on ferrihydrite: kinetics, equilibrium, and adsorption envelopes. *Environ. Sci. Technol.* **1998**, *32*, 344–349.
- (18) Masue, Y.; Loeppert, R. H.; Kramer, T. A. Arsenate and arsenite adsorption and desorption behavior on coprecipitated aluminum: Iron hydroxides. *Environ. Sci. Technol.* **2007**, *41*, 837–842.
- (19) Anderson, M. A.; Ferguson, J. F.; Gavis, J. Arsenate adsorption on amorphous aluminum hydroxide. *J. Colloid Interface Sci.* **1976**, *54*, 391–399.
- (20) Gupta, S. K.; Chen, K. Y. Arsenic removal by adsorption. *J. Water Pollut. Control Fed.* **1978**, *50*, 493–506.
- (21) Hingston, F. J. In *Adsorption of Inorganics at Solid-Liquid Interfaces*; Anderson, M. A.; Rubin, A. J., Eds.; Ann Arbor Science: Ann Arbor, MI, 1981; pp 51–90.
- (22) Foster, A. L.; Brown, G. E.; Parks, G. A. X-ray absorption fine structure study of As (V) and Se (IV) sorption complexes on hydrous Mn oxides. *Geochim. Cosmochim. Acta* **2003**, *67*, 1937–1953.
- (23) Manning, B. A.; Fendorf, S. E.; Bostick, B.; Suarez, D. L. Arsenic(III) oxidation and arsenic(V) adsorption reactions on synthetic birnessite. *Environ. Sci. Technol.* **2002**, *36*, 976–981.
- (24) Lafferty, B. J.; Ginder-Vogel, M.; Zhu, M.; Livi, K. J. T.; Sparks, D. L. Arsenite oxidation by a poorly crystalline manganese-oxide. 2. Results from X-ray absorption spectroscopy and X-ray diffraction. *Environ. Sci. Technol.* **2010**, *44*, 8467–8472.
- (25) Tani, Y.; Miyata, N.; Ohashi, M.; Ohnuki, T.; Seyama, H.; Iwahori, K.; Soma, M. Interaction of inorganic arsenic with biogenic manganese oxide produced by a Mn-oxidizing fungus, strain KR21–2. *Environ. Sci. Technol.* **2004**, *38*, 6618–6624.
- (26) Drits, V. A.; Silvester, E.; Gorshkov, A. I.; Manceau, A. Structure of synthetic monoclinic Na-rich birnessite and hexagonal birnessite: I. Results from X-ray diffraction and selected-area electron diffraction. *Am. Mineral.* **1997**, *82*, 946–961.
- (27) Silvester, E.; Manceau, M.; Drits, V. A. Structure of synthetic monoclinic Na-rich birnessite and hexagonal birnessite: II. Results from chemical studies and EXAFS spectroscopy. *Am. Mineral.* **1997**, *82*, 962–978.
- (28) Marcus, M. A.; Manceau, A.; Kersten, M. Mn, Fe, Zn and As speciation in a fast-growing ferromanganese marine nodule. *Geochim. Cosmochim. Acta* **2004**, *68*, 3125–3136.
- (29) Peacock, C. L.; Sherman, D. M. Sorption of Ni by birnessite: Equilibrium controls on Ni in seawater. *Chem. Geol.* **2007**, *238*, 94–106.
- (30) Manceau, A.; Tommaseo, C.; Rihs, S.; Geoffroy, N.; Chateigner, D.; Schlegel, M.; Tisserand, D.; Marcus, M. A.; Tamura, N.; Chen, Z. S. Natural speciation of Mn, Ni, and Zn at the micrometer scale in a clayey paddy soil using X-ray fluorescence, absorption, and diffraction. *Geochim. Cosmochim. Acta* **2005**, *69*, 4007–4034.
- (31) Manceau, A.; Lanson, M.; Geoffroy, N. Natural speciation of Ni, Zn, Ba, and As in ferromanganese coatings on quartz using X-ray fluorescence, absorption, and diffraction. *Geochim. Cosmochim. Acta* **2007**, *71*, 95–128.
- (32) Toner, B.; Manceau, A.; Webb, S. M.; Sposito, G. Zinc sorption to biogenic hexagonal-birnessite particles within a hydrated bacterial biofilm. *Geochim. Cosmochim. Acta* **2006**, *70*, 27–43.
- (33) Pena, J.; Kwon, K. D.; Refson, K.; Bargar, J. R.; Sposito, G. Mechanisms of nickel sorption by a bacteriogenic birnessite. *Geochim. Cosmochim. Acta* **2010**, *74*, 3076–3089.
- (34) Villalobos, M.; Bargar, J.; Sposito, G. Mechanisms of Pb(II) sorption on a biogenic manganese oxide. *Environ. Sci. Technol.* **2005**, *39*, 569–576.
- (35) Parikh, S. J.; Lafferty, B. J.; Sparks, D. L. An ATR-FTIR spectroscopic approach for measuring rapid kinetics at the mineral/water interface. *J. Colloid Interface Sci.* **2008**, *320*, 177–185.
- (36) Jackson, B. P.; Miller, W. P. Effectiveness of phosphate and hydroxide for desorption of arsenic and selenium species from iron oxides. *Soil Sci. Soc. Am. J.* **2000**, *64*, 1616–1622.
- (37) Lafferty, B. J.; Loeppert, R. H. Methyl arsenic adsorption and desorption behavior on iron oxides. *Environ. Sci. Technol.* **2005**, *39*, 2120–2127.
- (38) Liu, F.; De Cristofaro, A.; Violante, A. Effect of pH, phosphate and oxalate on the adsorption/desorption of arsenate on/from goethite. *Soil Sci.* **2001**, *166*, 197–208.
- (39) Zhu, M.; Paul, K. W.; Kubicki, J. D.; Sparks, D. L. Quantum chemical study of arsenic (III, V) adsorption on Mn-oxides: Implications for arsenic(III) oxidation. *Environ. Sci. Technol.* **2009**, *43*, 6655–6661.
- (40) Drits, V. A.; Lanson, B.; Gaillot, A. C. Birnessite polytype systematics and identification by powder X-ray diffraction. *American mineralogist* **2007**, *92*, 771.
- (41) Murray, J. W. The interaction of metal ions at the manganese dioxide-solution interface. *Geochim. Cosmochim. Acta* **1975**, *39*, 505–519.
- (42) Tonkin, J. W.; Balistrieri, L. S.; Murray, J. W. Modeling sorption of divalent metal cations on hydrous manganese oxide using the diffuse double layer model. *Appl. Geochem.* **2004**, *19*, 29–53.